

Modelling Low Field Electron Mobility In Group III Nitride Materials

¹M. Tohidi, ²F. Z. Tohidi, ³P. Ashori and ³H. Arabshahi

¹Department of Medical Physics, Birjand University of Medical Science, Birjand, Iran

²Physics Department, Payame Noor University of Mashhad, Mashhad, Iran

³Physics Department, Payame Noor University of Fariman, Fariman, Iran

Abstract

Temperature and doping dependencies of electron mobility in both wurtzite and zincblende GaN structures have been calculated using an iterative technique. The following scattering mechanisms, i.e. impurity, polar optical phonon, acoustic phonon, piezoelectric and electron plasmon are included in the calculation. Ionized impurity scattering has been treated beyond the Born approximation using the phase-shift analysis. It is found that the electron mobility decreases monotonically as the temperature increases from 100K to 600K. The low temperature value of electron mobility increases significantly with increasing doping concentration. The iterative results are in fair agreement with other recent calculations obtained using the relaxation-time approximation and experimental methods.

Keywords: GaN; SiC; Wurtzite; Zincblende; Plasmon

I. Introduction

Wide band gap GaN and related compounds with aluminium and indium currently have two main uses in commercial devices, providing bright LEDs emitting at ultraviolet-blue green wavelengths for CD-ROM and sensor applications and heterojunction field effect transistors (HFETs) which can sustain high current densities at elevated temperatures [1-2]. It has been shown that GaN has large peak electron velocity and can be an important candidate for high frequency application. A wide energy band gap leads to a low intrinsic carrier concentration, which enables a more precise control of free carrier concentration over a wide range of carrier concentration over a wide range of temperatures, and hence the devices made of this kind of material will be operable at high temperatures with large breakdown voltage. The development of GaN based transport devices is hampered by the nonavailability of detailed knowledge of the transport properties and transport parameter. Keeping in mind its huge technological prospect, we need a better understanding of these materials. The electron drift mobility is the most popular and important transport parameter used to characterize the microscopic quality of epitaxial layers. There has

been very little work on the calculation of low field electron mobility in GaN, Chin et al. [3] have used the variational principle to calculate low field electron mobilities and compared their results with fairly old experimental data. They have tried to fit the experimental data with an overestimated compensation ratio. In old samples, low electron mobility was due to poor substrate and buffer quality and other growth related problems. The iterative technique has been used by Rode and Gaskill [4] for low field electron mobility in GaAs for the dependence of mobility on electron concentration, but not on temperature, and ionized impurity scattering has been estimated within the Born approximation, which might be the reason for poor fitting at high electron concentrations.

This paper presents the iterative calculation results of electron transport in bulk GaN for both the natural wurtzite and also the zincblende lattice phases. Most of the calculations have been carried out using a non-parabolic ellipsoidal valley model to describe transport in the conduction band. However, the simpler and less computationally intensive spherical parabolic band scheme has also been applied, to test the validity of this approximation. The iterative calculations take into account the electron-lattice interaction through polar optical phonon scattering, deformation potential acoustic phonon scattering (treated as an elastic process), piezoelectric and electron plasmon scattering. Impurity scattering due to ionized and neutral donors is also included, with the latter found to be important at low temperature due to the relatively large donor binding energy which implies considerable carrier freeze-out already at liquid nitrogen temperature.

This paper is organized as follows. Details of the iterative model and the electron mobility calculations are presented in section II, the electron scattering mechanism which have been used are discussed in section III and the results of iterative calculations carried out on GaN structures are interpreted in section IV.

II. Model details

In principle the iterative technique give exact numerical prediction of electron mobility in bulk semiconductors. To calculate mobility, we have to solve the Boltzmann equation to get the modified

probability distribution function under the action of a steady electric field. Here, we have adopted the iterative technique for solving the Boltzmann transport equation. Under application of a uniform electric field the Boltzmann equation can be written as

$$\left(\frac{e}{\hbar}\right)E \cdot \nabla_k f = \int [s' f'(1-f) - s f(1-f')] dk \quad (1)$$

where $f = f(k)$ and $f' = f(k')$ are the probability distribution functions and $s = s(k, k')$ and $s' = s(k', k)$ are the differential scattering rates. If the electric field is small, we can treat the change from the equilibrium distribution function as a perturbation which is first order in the electric field. The distribution in the presence of a sufficiently small field can be written quite generally as

$$f(k) = f_0(k) + g(k) \cos \theta \quad (2)$$

where $f_0(k)$ is the equilibrium distribution function, θ is the angle between k and E and $g(k)$ is an isotropic function of k , which is proportional to the magnitude of the electric field. In general, contributions to the differential scattering rates come from two types of scattering processes, elastic scattering s_{el} , due to acoustic, impurity, plasmon and piezoelectric phonons, and inelastic scattering s_{inel} , due to polar optic phonons

$$s(k, k') = s_{el}(k, k') + s_{inel}(k, k') \quad (3)$$

The polar phonon energy is quite high (~92 meV) in case of GaN. Hence, this scattering process can not be treated within the framework of the relaxation time approximation (RTA) because of the possibility of the significant energy exchange between the electron and the polar optic modes. In this case, s_{inel} represents transitions from the state characterized by k to k' either by emission [$s_{em}(k, k')$] or by absorption [$s_{ab}(k, k')$] of a phonon. The total elastic scattering rate will be the sum of all the different scattering rates which are considered as elastic processes, i.e. acoustic, piezoelectric, ionized impurity, and electron-plasmon scattering. In the case of polar optic phonon scattering, we have to consider scattering-in rates by phonon emission and absorption as well as scattering-out rates by phonon absorption and emission. Using Boltzmann equation and considering all differential scattering rates, the factor $g(k)$ in the perturbed part of the distribution function $f(k)$ can be given by

$$g(k) = \frac{-eE \frac{\partial f_0}{\partial k} + \sum \int g' \cos \phi [s_{inel}'(1-f) + s_{inel} f]}{\sum \int (1 - \cos \phi) s_{el} dk + \sum \int [s_{inel}(1-f') + s_{inel}' f']} dk \quad (4)$$

Note, the first term in the denominator is simply the momentum relaxation rate for elastic scattering. It is

interesting to note that if the initial distribution is chosen to be the equilibrium distribution, for which $g(k)$ is equal zero, we get the relaxation time approximation result after the first iteration. We have found that convergence can normally be achieved after only a few iterations for small electric fields. Once $g(k)$ has been evaluated to the required accuracy, it is possible to calculate quantities such as the drift mobility which is given by

$$\mu_d = \frac{\hbar \int_0^\infty k^3 \frac{g(k)}{Ed} dk}{3m \int_0^\infty k^2 f(k) dk} \quad (5)$$

Where d is defined as $1/d = m \nabla_k E / \hbar^2 k$. In the following section electron-phonon, electron-impurity and electron-plasmon scattering mechanisms will be discussed.

III. Electron scattering mechanisms

A. Phonon scattering

The dominant scattering mechanism of electrons in polar semiconductors like GaN comes from the electron-phonon interaction except at the lowest temperatures. The electron-optical phonon interaction contributes both in the ohmic and non-ohmic mobility and provides the dominant energy-loss mechanism of electrons. First order polarization occurs in connection with the primitive unit cell, characteristic of the longitudinally polarized optical mode. In GaN the Debye temperature is more than 1000K [6], hence polar optical phonon scattering must be considered as an inelastic process. Other phonon scattering processes, i.e. acoustic and piezoelectric scattering are considered as elastic processes. Like GaAs, GaN also has a single minimum valley at $K=0$ (Γ valley). So internally phonon scattering can be neglected at low field conditions. In polar optic phonon scattering the differential scattering rates for absorption and emission can be written as [5]

$$S_{op}(k, k') = \frac{\sqrt{2m^*} e^2 \omega_{op}}{8\pi \epsilon_0 \hbar} \left(\frac{1}{\epsilon_\infty} - \frac{1}{\epsilon_s} \right) \frac{1 + 2\alpha E'}{\gamma^{1/2}(E)} F_0(E, E') \{N_{op}, (N_{op} + 1)\} \quad (6)$$

where ϵ_s and ϵ_∞ are define in table 1, N_{op} is the phonon occupation number and the N_{op} and $1+N_{op}$ refer to absorption and emission, respectively. For small electric fields, the phonon population will be very close to equilibrium, so that the average number of phonons is given by the Bose-Einstein distribution function. We have found that after a few iterations, the electron polar optical phonon scattering rate converges and becomes very close to the experimental result [6]. Also it is found that the electron polar optical phonon scattering rate in GaN

is almost one order of magnitude larger than in GaAs, which can be attributed to its larger ionic properties. The energy range involved in the case of scattering by acoustic phonons is from 0 to $2\hbar v_s k$, as the momentum conservation restricts the phonon wave vector q between 0 and $2k$, where k is the electron wave vector. Typically the average value of k is on the order of 10^7 cm^{-1} and v_s , the velocity of sound in the medium, is on the order of 10^5 cm/s . Hence, $2\hbar v_s k \approx 1 \text{ meV}$, which is small compared to the thermal energy. Hence electron-acoustic phonon scattering can be considered as an elastic process. Actually, a long wave length acoustic displacement can not affect the energy since neighboring unit cells move by almost the same amount, only the differential displacement (normally the strain) is of importance. The total differential scattering rate for acoustic phonons can be given by

$$S_{ac}(k, k') = \frac{\sqrt{2} D_{ac}^2 (m_i^* m_j^*)^{1/2} K_B T}{\pi \rho v^2 \hbar^4} \left[\frac{\sqrt{E(1+\alpha E)}}{(1+2\alpha E)} [(1+\alpha E)^2 + 1/3(\alpha E)^2] \right] \quad (7)$$

where D_{ac} is the acoustic deformation potential, ρ is the material density and α is the non-parabolicity coefficient. The formula clearly shows that the acoustic scattering increases with temperature. In crystals like GaN, whose lattice lacks inversion symmetry, such as those semiconductors with sphacelate or wurtzite structure, elastic strain may be accompanied by macroscopic electric fields. This piezoelectric effect provides an additional coupling between the electric and acoustic vibrations. The differential scattering rate for piezoelectric scattering will be

$$S_{pz}(k, k') = \frac{\sqrt{m^*} e^2 K_{ac}^2 K_B T}{4\sqrt{2} \pi \epsilon_0 \epsilon_s \hbar^2} \gamma^{-1/2}(E) (1+2\alpha E)^2 \times \ln\left(1 + \frac{8m^* \gamma(E)}{\hbar^2 q_0^2}\right) \quad (8)$$

where K_{av} is the dimensionless so called average electromechanical coupling constant [7].

B. Impurity scattering

The standard technique for dealing with ionized impurity scattering in semiconductors is the Brook-Herring (BH) technique [8], which is based on two inherent approximations. First, is the first order Born approximation and second is the single ion screening approximation. These two approximations essentially lead to a poor fit to the experimental mobility data [9,10]. Several attempts have been made to modify the BH technique phenomenologically [11]. It has been shown that phase-shift analysis of electron-impurity scattering is the best way to overcome the Born approximation. Departure from the BH prediction of electron mobility is evident at higher electron concentrations.

Meyer and Bartoli [9] have provided an analytic treatment based on phase-shift analysis taking into account the multi-ion screening effect and finally been able to overcome both the approximations. All the previous techniques of impurity screening by free electrons in semiconductors were based on the Thomas-Fermi (TF) approximation which assures that a given impurity should be fully screened. The breakdown of the single-ion screening formalism becomes prominent in the strong screening regime, where the screening length calculated through TF theory becomes much shorter than the average distance between the impurities and hence neighboring potentials do not overlap significantly. This essentially leads to a physically unreasonable result. In the case of high compensation, the single-ion screening formalism becomes less relevant, because in order to maintain the charge neutrality condition, it would be more difficult for a given number of electrons to screen all the ionized donors separately. In the case of GaN, the compensation ratio is usually quite large, and the ratio N_D^+/n is also temperature dependent. Hence the multi-ion screening correction is very essential in GaN. The effective potential of an ionized impurity scattering center is spherically symmetric in nature, so one can use phase-shift analysis to find the differential scattering rate $s(k, k')$ more accurately. The effective potential $V(r)$ due to an ionized impurity can be expressed as $V(r) = -(Z_i e^2) / (4\pi \epsilon_0 \kappa_0 r) e^{-r/\lambda}$, where Z_i is the charge of the ionized impurity in units of e and λ is the screening length. The standard technique to find out the screening length is the TF approach which is based on single ion screening approximation. In TF one can calculate the charge contribution q_i to the screening of a single ionized donor by an electron of energy E_i and is given by $q_i = -(2e^3 \lambda^2 / \epsilon_0 \kappa_0 E_i V)$. In the case of multi-ion problem, the TF approach can be generalized to find out the effective charge contribution due to an electron to screen all ionized donors and can be given by $Q_i = -(2e^3 N_D^+ \lambda^2 / \epsilon_0 \kappa_0 E_i)$. Total screening charge exactly neutralizes the ionized donors, when Q_i is summed over all electronic states

$$\sum_i -\frac{Q_i}{e} f_0(E_i) = N_D^+ \quad (9)$$

For the sufficiently low energy electrons, Q_i can be greater than the electronic charge, which is physically unreasonable. One way to tackle [9] this problem is to introduce a factor S_i such that

$$S_i(E_i) = \frac{E_i}{\xi} \quad E_i < \xi \quad (10)$$

where $\xi = (2N_D^+ e^2 \lambda^2 / \epsilon_0 \kappa_0)$, Q_i will be modified to $Q_i' = Q_i S_i$ in Eq. (9). For the low energy electrons the contribution will be $-e$. Since the total contribution to the screening by the low energy electrons has been effectively decreased, Eq. (9) no longer holds.

However, if the screening length λ is more than the average distance between the donors, it is not necessary to insist that each donor be fully screened, only it is required that overall charge neutrality should be preserved. Electrons in the overlap region can provide screening to both the ionized donors. Here we can define a factor p , which would be the fraction of the total charge, which is contained within a sphere of radius R surrounding the donor. Hence Eq. (9) will be modified as

$$\sum_i -\frac{Q_i}{e} f_0(E_i) = pN_d^+ \quad (11)$$

where $Q_i = pQ_d S_i$. The screening charge requirement will be fulfilled by adjusting the screening length until Eq. (11) is satisfied and is given by

$$\lambda_m^{-2} = \eta \lambda_0^{-2} \quad (12)$$

where λ_m is multi-ion screening length and λ_0 is TF screening length. The differential scattering rate for ionized impurity can be given as

$$S_{ii}(k, k') = \frac{8\pi^3 \hbar^3}{m^2 v^2} |f(X)|^2 \delta[E(k') - E(k)] \quad (13)$$

where scattering amplitude $f(X)$ depends on the phase shift δ_1 and Legendre polynomial P_1 and is given by

$$f(X) = \frac{1}{2ik} \sum_{l=0}^{\infty} (2l+1)(e^{2i\delta_l} - 1)P_l(X) \quad (14)$$

It has already been mentioned that in n-type GaN the activation energy of the donors is quite large, which keeps a large number of donors neutral at low temperatures. Neutral impurity scattering has been dealt with previously using the Erginsoy [12] expression which is based on electron scattering by a hydrogen atom and a scaling of the material parameters. It has been shown that an error as high as 45% results in the neutral impurity scattering cross section with this simple model. Meyer and Bartoli [9] have given a phase shift analysis treatment based on the variational results of Schwartz [13] to calculate the neutral impurity cross section, which is applicable for a larger range of electron energy.

C. Plasmon scattering

Though carrier mobility and various scattering phenomena in semiconductor have been studied extensively, there is hardly any study regarding the effect of electron-plasmon scattering on electron mobility except the excellent work by Fischetti in the case of Si [14]. He has shown that the electron-plasmon interaction is important at doping densities above 10^{17} cm^{-3} . Plasmons are the collective excitations of the free electrons against the positive background charges, and create long range electric fields (like LO polar optic phonons) which can scatter the electrons. In the case of electron-plasmon scattering, electrons can gain momentum from collective excitations, but it may be returned to

electrons if plasmons decay into single particle excitations, which is called Landau damping. Electron mobility is affected indirectly by modifying the distribution function if Landau damping is the faster decay channel. When plasmons decay through collisions with phonons and impurities, it can directly affect the electron mobility. It has been shown [14] that if decay due to collisional damping dominates over Landau damping, electron-plasmon scattering can reduce the electron mobility by 20% for electron concentrations greater than 10^{17} cm^{-3} . The differential scattering rate for an electron of wave vector k and energy E to absorb or emit a plasmon of energy $\hbar\omega$ is given by

$$S_{e-p}(k, k') = \Theta(E') \frac{\omega k' (1 + 2\alpha E')}{a_0} \frac{1 - f_0(E')}{1 - f_0(E)} \quad (15)$$

$$\left(N_p(\omega) + \frac{1}{2} \mp \frac{1}{2} \right) \times \int \left(1 - \frac{k' \phi(E')}{k \phi(E)} X \right) \frac{1}{q^2} dX$$

where upper and lower signs represent absorption and emission, respectively. $X_c = [1 + \Psi - (q_c/k)^2 / 2\Psi^{1/2}]$, q_c is the maximum value of the plasmon wave vector, above which plasma oscillation can not be sustained. The usual approximation is $q_c = 1/\lambda_0$. $\Theta(E')$ is the step function, where $E' = E \pm \hbar\omega$, $N_p(\omega) = 1/[\exp(\hbar\omega/k_B T) - 1]$ is the Bose occupation number of the plasmons. q is the plasmon wave vector given by $q^2 = k^2(1 + \Psi - 2\Psi^{1/2}X)$ and

$$\Psi = (k'/k)^2 = (1 \pm \hbar\omega/E)(1 + \alpha E').$$

$\phi(E) = \tau(E)/(1 + 2\alpha E)$, where $\tau(E)$ is the total relaxation time. To evaluate the integral in Eq.15 requires the solution of the nonlinear Boltzmann equation. It has been shown [8] that the energy dependence of ϕ can be ignored for the entire electron concentration range of interest, which means that $\phi(E)/\phi(E) \approx 1$. The total plasmon momentum relaxation rate is given by

$$\nu_{e-p} = \int_0^{\infty} g(\omega_p - \omega) \frac{1}{\tau_{pl}(E, \hbar\omega)} d(\hbar\omega) \quad (16)$$

where $\omega_p = \omega_{p0}(1 - 3\alpha\hbar\omega_{p0})$ is the plasma frequency corrected for the nonparabolicity effect and $\omega_{p0}^2 = ne^2 / \epsilon n^*$ is the plasma frequency.

$g(\omega_p - \omega) = \Gamma / \pi[(\hbar\omega_p - \hbar\omega)^2 + \Gamma^2]$, where Γ is the half width of the plasmon line due to Landau damping and is small at large impurity concentrations because the decay rate is inversely proportional to the plasma energy. The half width due to collision damping can be estimated by the single particle relaxation rate. We do not need to determine relaxation rate exactly, because mobility depends very weakly on Γ as long as the damping is not too strong.

IV. Results and discussion

We have performed a series of low-field electron mobility calculations for both the natural wurtzite and the zincblende lattice phases of GaN. Low-field mobilities have been derived using

iteration method. Important parameters used throughout the calculations are listed in table 1, which are taken from Ref. [15].

Figure 1 shows reasonably good agreement between experimental and calculated mobility-temperature dependencies in both structures. For wurtzite structure the calculations have been performed for an electric field applied along the Γ -A (c-axis, c-GaN) and Γ -M (parallel to basal plane, h-GaN) directions of the Brillouin zone. The peak electron drift mobility in two directions are, respectively, $1300 \text{ cm}^2/\text{V}\cdot\text{s}$ and $1100 \text{ cm}^2/\text{V}\cdot\text{s}$ at room temperature. The reason for this difference can be explained as follows. The Γ valley effective mass is greater in the Γ -M direction than Γ -A, which implies that an electric field applied perpendicular to the c-axis will be less efficient in heating the electron ensemble. It can be seen from the figure that the electron drift mobilities at room temperature that we find are 1300 and $1800 \text{ cm}^2/\text{V}\cdot\text{s}$ for wurtzite and zincblende structures, respectively, for an electric field equal to 10^4 Vm^{-1} and with a donor concentration of 10^{22} cm^{-3} . The results plotted in figure 1 indicate that the electron drift mobility of wurtzite GaN is lower than zincblende structure at all temperatures. This is largely due to the higher Γ valley effective mass in the wurtzite phase.

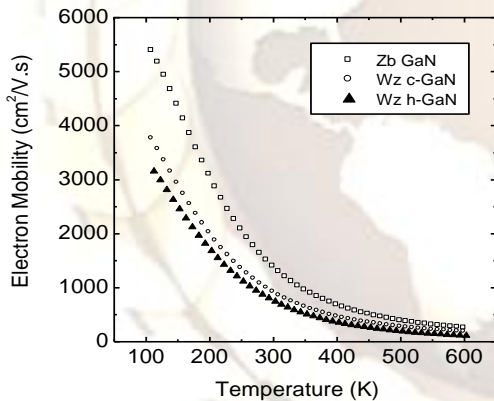
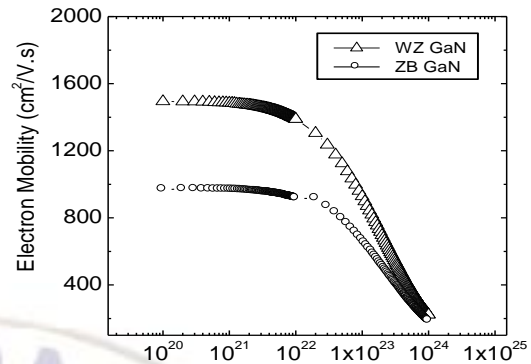


Fig.1. Electron drift mobility of GaN in zincblende and wurtzite structures (both perpendicular to c-axis and parallel to c-axis) versus temperature. Donor concentration is approximately 10^{22} cm^{-3} .

Figure 2 shows the calculated variation of the electron mobility as a function of the donor concentration for both GaN crystal structures at room temperature. The mobility does not vary monotonically between donor concentrations of 10^{21} cm^{-3} and 10^{25} cm^{-3} due to the dependence of electron scattering on donor concentration, but shows a maximum near 10^{21} cm^{-3} for zincblende and wurtzite.



IEE REVIEW (Conf. Proc., Vol. 129, I, No. 1, DECEMBER 2003)

In figure 3, the electrons as a function of temperature using the screened shallow donor binding energy results of Wang, et al. [15] for different background electron concentrations. The temperature effects on the carrier screening are taken into account for this calculation. The figure clearly shows that for uncompensated GaN at liquid nitrogen temperature there is a large fraction of neutral donor impurities present.

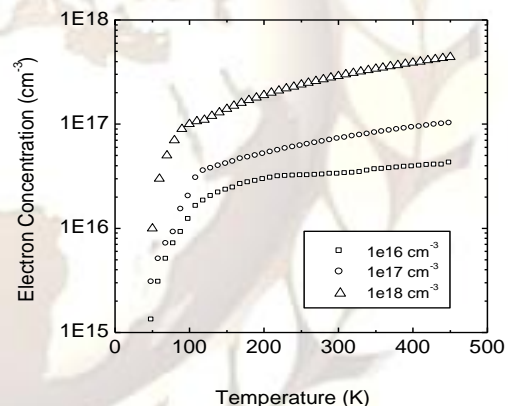
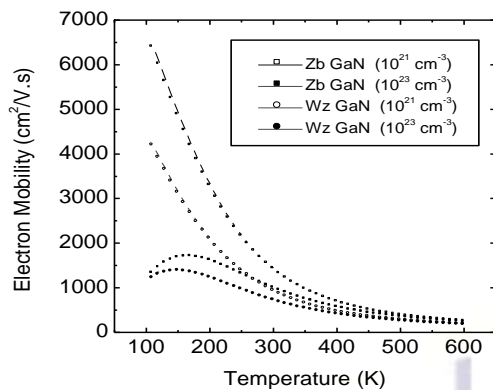


Fig.3. Electron concentration versus temperature for c-GaN with different donor doping densities.

The temperature variation of the electron drift mobility in zincblende and wurtzite GaN (c-GaN) for different donor concentrations is shown in figure 4. It is evident from this figure that the curves approach each other at very high temperatures, where the mobility is limited by longitudinal optical phonon scattering, whereas the mobility varies inversely with donor concentration at low temperature, as we would expect from the foregoing discussion. The decrease in mobility at low temperature is caused in part by neutral impurity scattering. For the lowest doping concentration considered in this calculation, 10^{21} cm^{-3} , we find that the neutral impurity scattering plays a large role at low temperature because of the significant carrier freeze-out evident from figure 3.



V. Summary

In conclusion, we have quantitatively obtained temperature-dependent and electron concentration-dependent electron mobility in both zincblende and wurtzite GaN structures using an iterative technique. The theoretical values show good agreement with recently obtained experimental data. It has been found that the low-field mobility is significantly higher for the wurtzite structure than zincblende due to the higher electron effective mass in the wurtzite crystal structure. Several scattering mechanisms have been included in the calculation including electron-plasmon scattering. Ionized impurities have been treated beyond the Born approximation using a phase shift analysis. Screening of ionized impurities has been treated more realistically using a multi-ion screening formalism, which is more relevant in the case of highly compensated III-V semiconductors like GaN and SiC.

References

- [1] S Nakamura, M Senoh and T Mukai, Appl. Phys. Lett. 62, 2390 (1993)
- [2] S Strite and H Morkoc, J. Vac. Sci. Technol. B 10, 1237 (1992)
- [3] V W L Chin and T L Tansley, J. Appl. Phys. 75, 7365 (1994)
- [4] D L Rode and D K Gaskill, Appl. Phys. Lett. 66, 1972 (1995)
- [5] C Moglestue, Monte Carlo simulation of semiconductor devices, Chapman and Hall (1993)
- [6] K T Tsen, D K Ferry, A Botchkarev, B Suerd, A Salvador and H Morkoc, Appl. Phys. Lett. 71, 1852 (1997)
- [7] B K Ridley, Electrons and phonons in semiconductor multilayers, Cambridge University press (1997)
- [8] H Brooks, Phys. Rev. 83, 879 (1951)
- [9] J R Meyer and F J Bartoli, Phys. Rev. B 23, 5413 (1981)
- [10] J R Meyer and F J Bartoli, Solid State State Commun. 41, 19 (1982)
- [11] D Chattopadhyya and H J Queisser, Rev. Mod. Phys. 53, 745 (1981)
- [12] C Erginsoy, Phys. Rev. 79, 1013 (1950)
- [13] C Schwartz, Phys. Rev. 124, 1468 (1961)
- [14] M V Fischetti, Phys. Rev. 44, 5527 (1991)
- [15] H Morkoc, Nitride semiconductor and devices, Springer-velag.